EVALUATION OF EFFECTS OF LWR COOLANT ENVIRONMENTS ON FATIGUE LIFE OF CARBON AND LOW-ALLOY STEELS*

Omesh K. Chopra and William J. Shack
Energy Technology Division,
Argonne National Laboratory,
Argonne, Illinois, 60439, USA

February 1996

To be presented at the Symposium on "Effects of the Environment on the Initiation of Crack Growth," May 20–21, 1996, Orlando, Florida

*Work supported by the Office of Nuclear Regulatory Research of the U.S. Nuclear Regulatory Commission, under FIN Number A2212; Program Manager: Dr. M. McNeil.

DISCLAIMER

Omesh K. Chopra[1] and William J. Shack[1]

EVALUATION OF EFFECTS OF LWR COOLANT ENVIRONMENTS ON FATIGUE LIFE OF CARBON AND LOW–ALLOY STEELS

REFERENCE: Chopra, O. K., and Shack, W. J., "**Evaluation of Effects of LWR Coolant Environments on Fatigue Life of Carbon and Low–Alloy Steels**," Effects of the Environment on the Initiation of Crack Growth, ASTM STP 1298, W. A. Van Der Sluys, R. S. Piascik, and R. Zawierucha, eds., American Society for Testing and Materials, Philadelphia, 1997.

ABSTRACT: The ASME Boiler and Pressure Vessel Code provides rules for the construction of nuclear power plant components. Figure I–90 of Appendix I to Section III of the Code specifies fatigue design curves for structural materials. However, the effects of light water reactor (LWR) coolant environments are not explicitly addressed by the Code design curves. Recent test data indicate a significant decrease in fatigue life of carbon and low–alloy steels in LWR environments when five conditions are satisfied simultaneously, viz., applied strain range, temperature, dissolved oxygen in the water, and sulfur content of the steel are above a minimum threshold level, and the loading strain rate is below a threshold value. Only a moderate decrease in fatigue life is observed when any one of these conditions is not satisfied. This paper summarizes available data on the effects of various material and loading variables such as steel type, dissolved oxygen level, strain range, strain rate, and sulfur content on the fatigue life of carbon and low–alloy steels. The data have been analyzed to define the threshold values of the five critical parameters. Methods for estimating fatigue lives under actual loading histories are discussed.

KEYWORDS: fatigue crack initiation, strain vs. life (S–N) curve, LWR environment, carbon steel, low–alloy steel, strain rate, dissolved oxygen, sulfur content

---

INTRODUCTION

Plain carbon and low–alloy steels are used extensively in light water reactor (LWR) steam supply systems as piping and pressure–vessel materials. The ASME Boiler and Pressure Vessel Code Section III, which contains rules for the construction of Class 1 components for nuclear power plants, recognizes fatigue as a possible mode of failure in pressure vessel steels and piping materials. Cyclic loadings on a structural component

---

[1]Metallurgist and Associate Director, respectively, Energy Technology Division, Argonne National Laboratory, Argonne, IL 60439

occur as a system moves from one load set (e.g., pressure, temperature, moment, and force loading) to any other load set. For each pair of load sets, an individual fatigue usage factor is determined by the ratio of the number of cycles anticipated during the lifetime of the component to the allowable cycles. Figure I–90 of Appendix I to Section III of the Code specifies fatigue design curves that define the allowable number of cycles as a function of applied stress amplitude. The cumulative usage factor (CUF) is the sum of the individual usage factors. The ASME Code Section III requires that the CUF at each location must not exceed a value of 1.

The current Code fatigue design curves are based on strain–controlled tests of small polished specimens at room temperature (RT) in air. In most studies, the fatigue life of a test specimen is defined as the number of cycles for the tensile stress to drop 25% from its peak value, which corresponds to a ≈3–mm–deep crack. Consequently, fatigue life N represents the number of cycles required to initiate a crack ≈3 mm deep. The best–fit curves to the experimental data are expressed in terms of the Langer equation [1]

$$\varepsilon_a = B(N)^{-b} + A, \qquad (1)$$

where ε_a is applied strain amplitude and A, B, and b are parameters of the model. The fatigue design curves were obtained by decreasing the best–fit curves to the experimental data by a factor of 2 on stress or 20 on cycles, whichever was more conservative, at each point on the best–fit curve. These factors are not safety margins but rather conversion factors that must be applied to the experimental data to obtain estimates of the lives of reactor components. The effect of LWR coolant environments on fatigue resistance of the material are not explicitly addressed in the Code design fatigue curves.

Recent fatigue strain vs. life (S–N) data from the U.S. [2–7] and Japan [8–12] illustrate potentially significant effects of LWR coolant environments on the fatigue resistance of carbon steels (CSs) and low–alloy steels (LASs). Environmental effects on fatigue life are significant when five conditions are satisfied simultaneously, viz., applied strain range, service temperature, dissolved oxygen (DO) in the water, and sulfur content of the steel are above a minimum threshold level, and the loading strain rate is below a threshold value. Although these are the minimum conditions that must be met to produce significant degradation in fatigue life, the actual dependence of fatigue life on these variables involves complex synergistic interactions. Also, studies on the effect of high–temperature aqueous environment on fatigue crack growth behavior of carbon and low–alloy steels indicate that flow rate is an important parameter for environmental effects on fatigue life in water [13,14]. However, experimental data to establish either the dependence of fatigue life on flow rate or the threshold flow rate for environmental effects on fatigue life are not available. When any one of the threshold conditions is not satisfied, environmental effects on fatigue life are modest. Interim fatigue design curves have been developed that take into account temperature, DO content in water, sulfur level in steel, and strain rate [15]. Statistical models have also been developed for estimating the effects of various material and loading conditions on fatigue life of materials used in the construction of nuclear power plant components [16]. Results of the statistical analysis have been used to estimate the probability of fatigue cracking in reactor components [16]. The Pressure Vessel Research Council (PVRC) has also been compiling and evaluating fatigue S–N data related to the effects of LWR coolant environments on the fatigue life of pressure boundary materials; the results have been presented by Van Der Sluys [17].

This paper summarizes available data on the effects of various material and loading variables such as steel type, dissolved oxygen level, strain range, strain rate, and sulfur

content on the fatigue life of CSs and LASs. The data have been analyzed to define the threshold values of the five critical parameters. Methods for evaluating the effects of LWR coolant environments on the fatigue life of these steels are presented, and estimations of fatigue lives under actual loading histories are discussed.

AIR ENVIRONMENT

The fatigue life of CSs and LASs in air depends on steel type, temperature, orientation, and strain rate. For LASs, the fatigue life is greater and fatigue endurance limit is higher than it is for CSs. For both steels, fatigue life decreases as temperature increases. Some steels show very poor fatigue properties in the transverse orientation. The fatigue lives of A302–Gr B steel in the rolling (R) and radial (T2) orientations are shown in Fig. 1. The fatigue life in the T2 orientation is nearly one order of magnitude lower than in the R orientation. Also, endurance limit in the T2 orientation is lower than it is in the R orientation. Metallographic examination of the specimens indicates that structural factors, such as distribution and morphology of sulfides, are responsible for the poor fatigue resistance of steels in transverse orientations, in which fatigue crack propagates preferentially along the sulfide stringers. The results also indicate that some heats of CS and LAS are sensitive to strain rate. For example, the fatigue life of A302–Gr B steel (Fig. 1) decreases with a decrease in strain rate. The effect of strain rate is quite significant for the T2 orientation. A similar strain rate effect has also been observed in A333–Gr 6 carbon steel [7]. However, two heats of CS and LAS showed no effect of strain rate on fatigue life in air at 288°C [5,6].

The cyclic stress–strain response of CSs and LASs varies with steel type and temperature. In general, these steels show initial cyclic hardening followed by cyclic softening or a saturation stage at all strain rates. Significant initial hardening is seen in the CSs with a pearlite and ferrite structure and low yield stress. The LASs, which consist of tempered ferrite and bainitic structure, have a relatively high yield stress, and show little or no initial hardening, may exhibit cyclic softening during testing. For both steels, maximum stress increases as applied strain increases and generally decreases as temperature increases. However, at 200–370°C, these steels exhibit dynamic strain aging, which results in enhanced cyclic hardening, a secondary hardening stage, and negative strain rate sensitivity [18–20]. The temperature range and extent of dynamic strain aging vary with composition and structure. Effect of strain rate and temperature on the cyclic stress of CSs and LASs is shown in Fig. 2. For both steels, cyclic stresses are

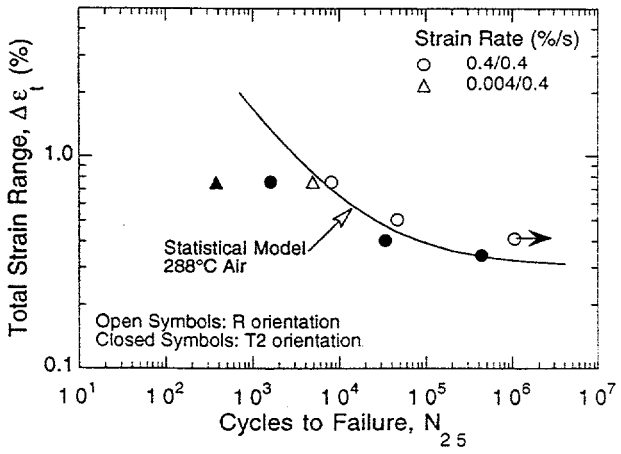

Figure 1— Effect of material orientation on fatigue life of A302–Gr B low–alloy steel in air

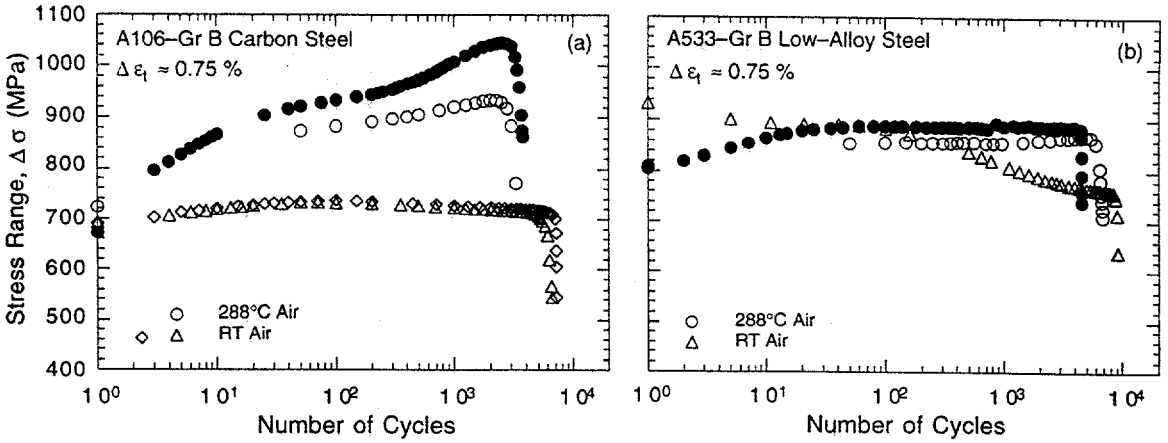

Figure 2—Effect of strain rate and temperature on cyclic stress of carbon and low–alloy steels in air

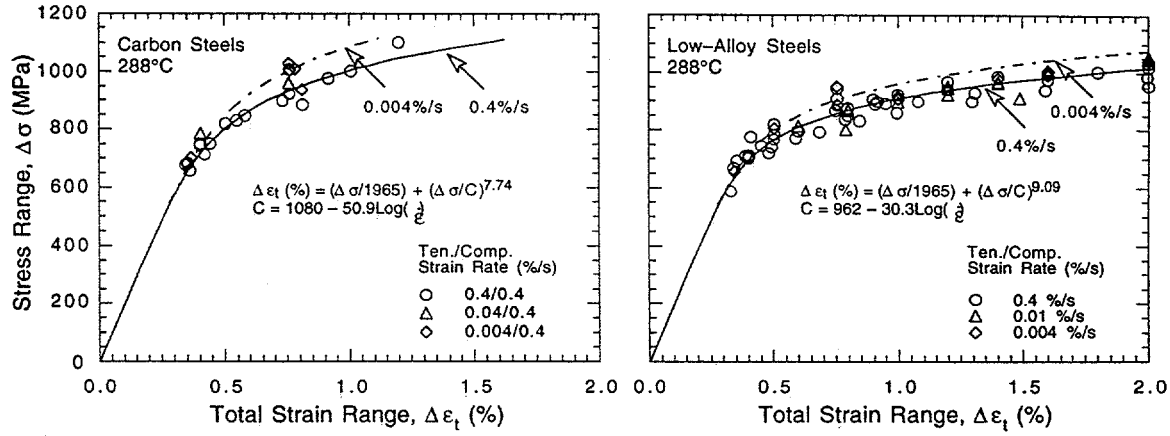

Figure 3—Cyclic stress–strain curve for carbon and low–alloy steels at 288°C in air

higher at 288°C than at room temperature. At 288°C, all steels exhibit greater cyclic and secondary hardening. The extent of hardening increases as applied strain rate decreases.

The cyclic stress vs. strain curves for CSs and LASs at 288°C are shown in Fig. 3; cyclic stress corresponds to the value at half life. The total strain range $\Delta\varepsilon_t$ (%) for CSs can be represented in terms of the cyclic stress range $\Delta\sigma$ (MPa) and applied strain rate $\dot{\varepsilon}$ (%/s) with the equation

$$\Delta\varepsilon_t = \frac{\Delta\sigma}{1965} - \left(\frac{\Delta\sigma}{C}\right)^{7.74}, \tag{2a}$$

where the constant C is expressed as

$$C = 1080 - 50.9\,\mathrm{Log}(\dot{\varepsilon}); \tag{2b}$$

and for LASs, with the equation

$$\Delta\varepsilon_t = \frac{\Delta\sigma}{1965} - \left(\frac{\Delta\sigma}{D}\right)^{9.09}, \tag{3a}$$

where the constant D is expressed as

$$D = 962 - 30.3\mathrm{Log}(\dot{\varepsilon}). \tag{3b}$$

The fatigue life of CSs and LASs in air and LWR environments can be estimated from statistical models [18]. In air, the fatigue life N, defined as the number of cycles to form a 3–mm–deep crack, of CSs is expressed as

$$\ln(N) = 6.570 - 0.00133\,T - 1.871\,\ln(\varepsilon_a - 0.11) \tag{4a}$$

and that of LASs as

$$\ln(N) = 6.667 - 0.00133\,T - 1.687\,\ln(\varepsilon_a - 0.15), \tag{4b}$$

where ε_a is the strain amplitude in % and T is the temperature in °C. The fatigue lives of CSs and LASs in air at room temperature and 288°C are compared with the values estimated from Eqs. 4a and 4b in Fig. 4. The results indicate significant heat–to–heat variation. At 288°C, fatigue life may vary up to a factor of 5 above or below the mean

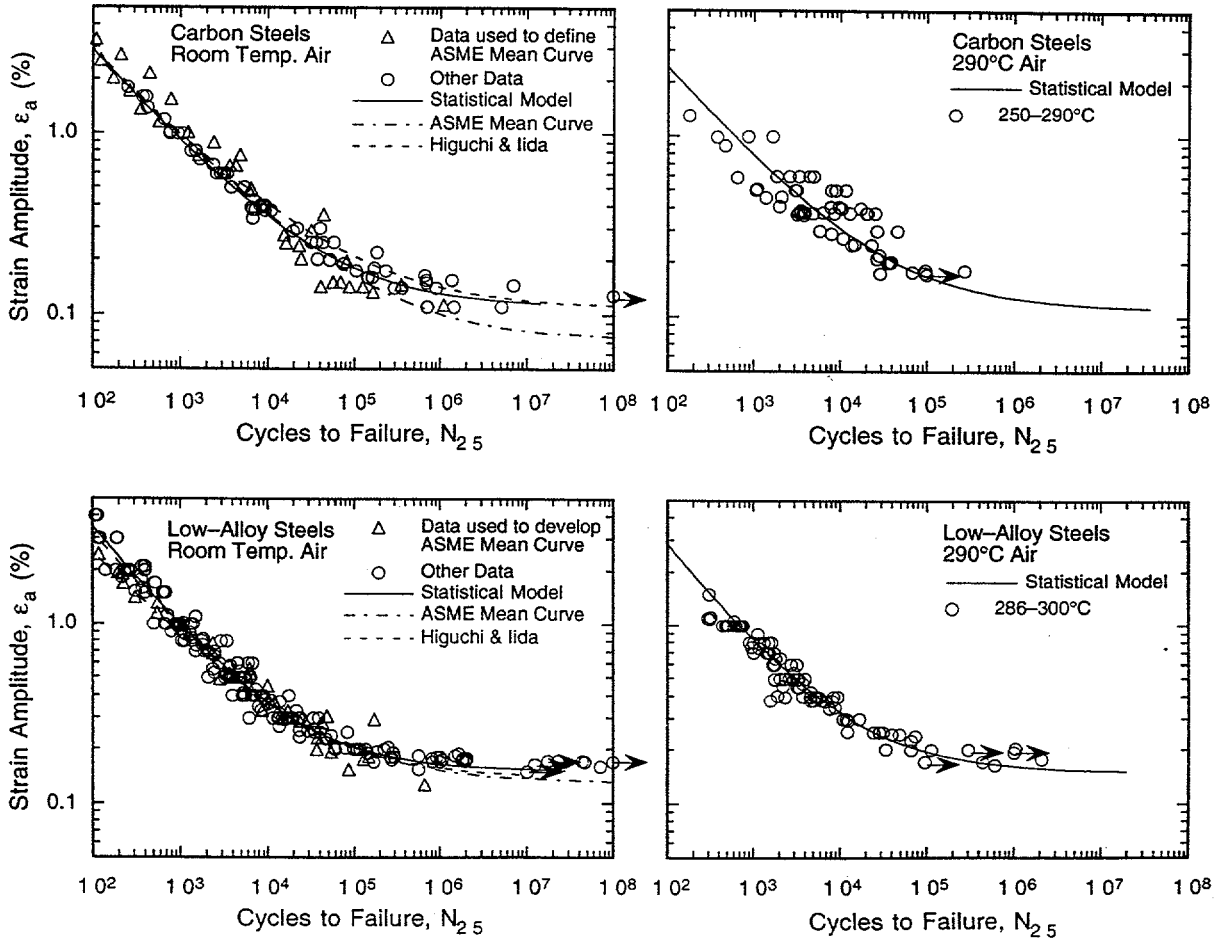

FIigure 4—Fatigue S–N behavior for carbon and low–alloy steels in air at room temperature and 290°C

value. The results also indicate that the ASME mean curve for CSs is not consistent with the experimental data; at strain amplitudes <0.2%, the mean curve predicts significantly lower fatigue lives than those observed experimentally. The estimated curve for LASs is comparable with the ASME mean curve. For both steels, Eq. 4 shows good agreement with the average curves of Higuchi and Iida [8]. The existing fatigue S–N data base for CSs and LASs does not include information regarding the size and distribution of inclusions in the steel. Consequently the effect of orientation could not be incorporated into the statistical model.

The fatigue data indicate that in the temperature range for dynamic strain aging, strain rate may influence fatigue life of some steels even in an inert environment; the fatigue life may be either unaffected [5,7], decrease for some heats [18,19], or increase for others [20]. The relatively large variation in life observed in the tests at 288°C may be due to differences in the extent of dynamic strain aging in the steel. Because of the conflicting possibilities, strain rate effects were not explicitly considered in the statistical model. Inhomogeneous plastic deformation can result in localized plastic strains, this localization retards blunting of propagating cracks that is usually expected when plastic deformation occurs and can result in higher crack growth rates [18]. The increases in fatigue life have been attributed to retardation of crack growth rates due to crack branching and suppression of plastic zone. Formation of cracks is easy in the presence of dynamic strain aging [20]. In an air environment, Eqs. 4a and 4b consider only the effects of steel type and temperature on fatigue life.

LWR ENVIRONMENTS

The fatigue data in LWR environments indicate a significant decrease in fatigue life of CSs and LASs when five conditions are satisfied simultaneously, viz., applied strain range, service temperature, DO in the water, and sulfur content of the steel are above a minimum threshold level, and the loading strain rate is below a threshold value. Although the microstructures and cyclic–hardening behavior of CSs and LASs are significantly different, environmental degradation of fatigue life of these steels is identical. For both steels, environmental effects on fatigue life are minimal if any one of these conditions is not satisfied. The effects of these parameters on fatigue life are discussed below in greater detail to define the threshold values.

Temperature

The change in fatigue life of two heats of A333–Gr 6 CS with test temperature at different levels of DO [8,9,12] is shown in Fig. 5. Other parameters, e.g., strain amplitude, strain rate, and sulfur content in steel, were kept constant; the applied strain amplitude and sulfur content were above and strain rate was below the critical threshold values. The results indicate a threshold temperature of 150°C, above which environment decreases fatigue life if DO in water is also above the critical threshold level. In the temperature range of 150–320°C, fatigue life decreases linearly with temperature; the decrease in life is greater at high temperatures and DO levels. Fatigue S–N data on high–sulfur LASs are inadequate to determine the temperature dependence of fatigue life in water. Available data indicate that the threshold value of 150°C and a linear dependence of fatigue life on temperature may also be applicable to LASs. At temperatures below the threshold value of 150°C, life in water is 30–50% lower than in RT air.

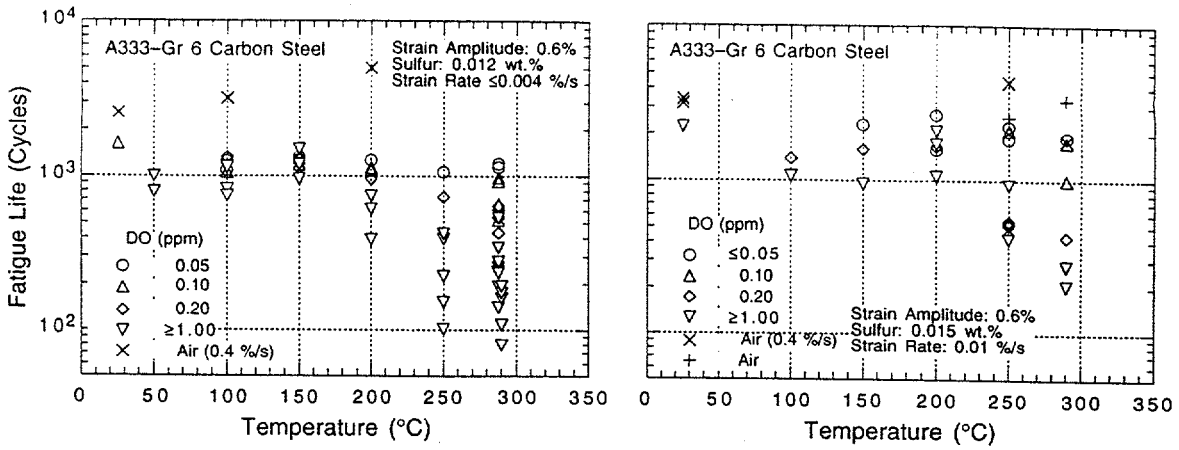

Figure 5—Change in fatigue life of A333–Gr 6 carbon steel with temperature and DO

Strain Rate

A slow strain rate applied during the tensile–loading cycle (slow/fast test) is primarily responsible for environmentally assisted reduction in fatigue life. Slow strain rate applied during both tensile– and compressive–loading cycles (slow/slow test) does not cause further decrease in fatigue life. However, limited data indicate that a slow strain rate during the compressive–loading cycle (fast/slow test) also decreases fatigue life, although the decrease in life is relatively small. The fatigue life of A533–Gr B steel at 288°C, 0.5–0.8 ppm DO, and ≈0.5% strain range decreased by factors of 5, 8, and 35 for the fast/fast, fast/slow, and slow/fast tests [5]. Similar results have been observed for A333–Gr 6 carbon steel; relative to the fast/fast test, fatigue life for slow/fast and fast/slow tests at 288°C, 8 ppm DO, and 1.2% strain range decreased by factors of 3.5 and 7.5, respectively [10].

The S–N data indicate that strain rates above 1 %/s have little or no effect on fatigue life of CSs and LASs in LWR environments. For strain rates <1 %/s, fatigue life decreases rapidly with decreasing strain rate. The fatigue lives of several heats of CSs and LASs [5–10] are plotted as a function of strain rate in Fig. 6. The results indicate that when threshold conditions for the five parameters are satisfied, fatigue life decreases with decreasing strain rate and increasing levels of DO in water and sulfur content in the steel. For both CSs and LASs, the effect of strain rate on fatigue life appears to saturate at ≈0.001%/s strain rate.

Dissolved Oxygen

The dependence of fatigue life of carbon steel on DO content in water [9,12] is shown in Fig. 7. The test temperature, applied strain amplitude, and sulfur content in steel were above, and strain rate was below, the critical threshold values. The results indicate a minimum DO level of 0.05 ppm, above which environment decreases fatigue life of the steel. The effect of DO content on fatigue life saturates at 0.5 ppm, i.e., increases in DO levels above 0.5 ppm do not cause further decreases in fatigue life. In Fig. 7, for DO levels between 0.05 and 0.5 ppm, fatigue life decreases logarithmically with DO. However, the data are extremely limited for adequate definition of the functional form for the dependence of life on DO content. The existing fatigue S–N data may also be represented by a linear dependence of life on DO content.

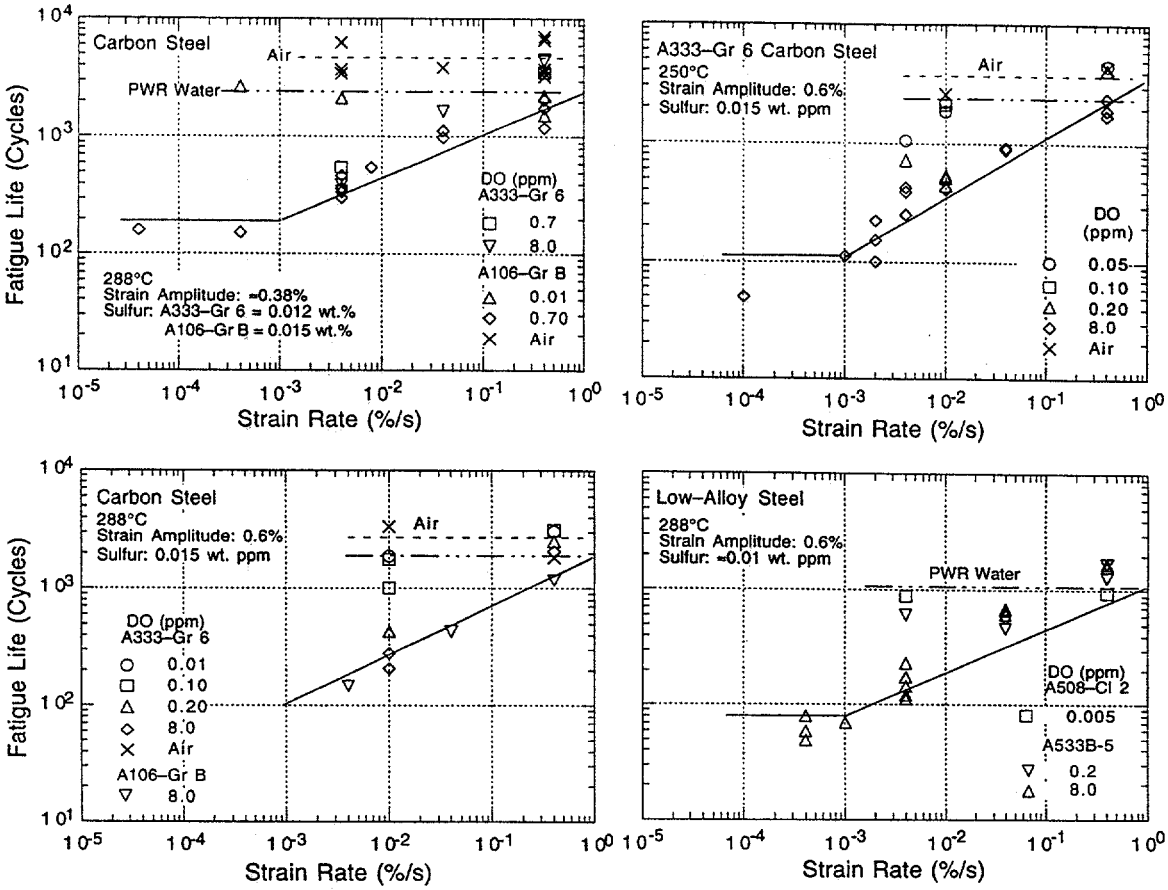

Figure 6—Dependence of fatigue life of several heats of carbon and low–alloy steels on strain rate at several dissolved oxygen levels

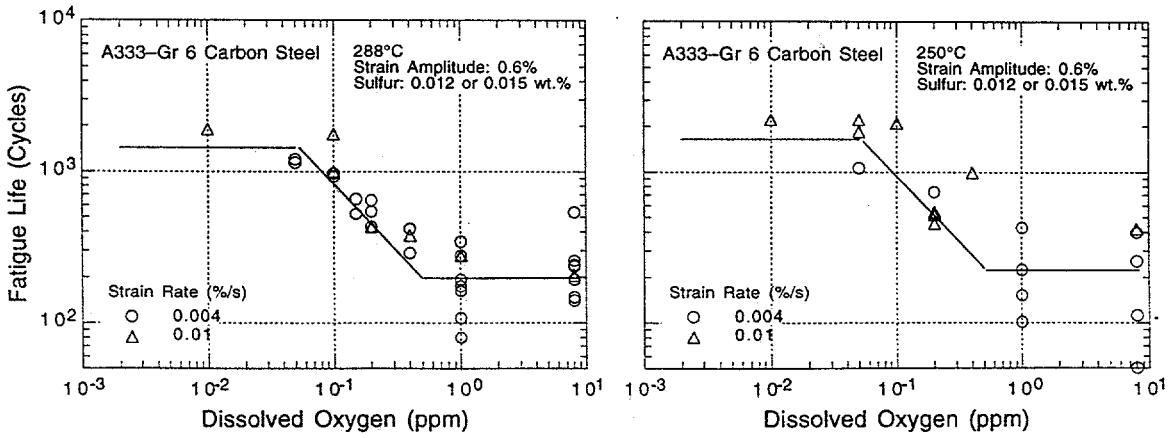

Figure 7—Dependence of fatigue life of carbon steel on dissolved oxygen

Low Dissolved Oxygen—Only a moderate decrease in fatigue life is observed in water when any one of the threshold conditions is not satisfied, e.g., low–DO pressurized water reactor (PWR) environments [4–8]. The fatigue life of CSs and LASs in simulated PWR water is shown in Fig. 8. For both steels, fatigue lives in a PWR environment are lower than those in air by a factor of less than 2. In PWR water, the effects of orientation and strain rate are similar to those in air. For some heats, a decrease in the strain rate by

three orders of magnitude does not cause an additional decrease in fatigue life, e.g., results for A106–Gr B and A533–Gr B steels in Fig. 8. On the other hand, for some heats, fatigue life decreased by a factor of ≈4 when strain rate decreased from 0.4 to 0.004%/s. The results also suggest that even the high–sulfur steels, e.g., A302–Gr B steel with 0.027 wt.% sulfur, which exhibit enhanced crack growth rates in PWR water [21], show only modest decreases of fatigue life in low–DO PWR water [5,7].

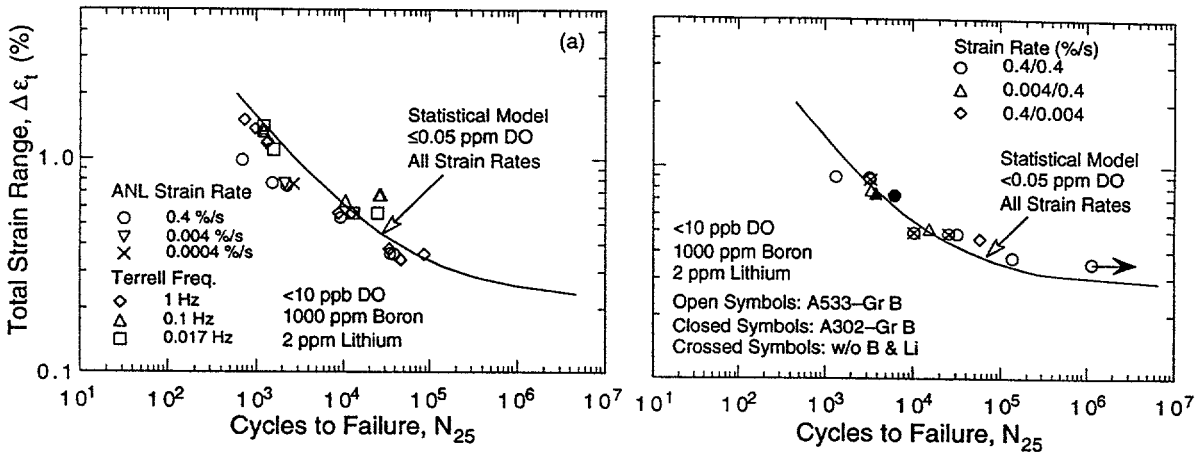

Figure 8—Fatigue S–N behavior for A106–Gr B and A533–Gr B steels estimated from model and determined experimentally in PWR water at 288 °C

Sulfur Content in Steel

The fatigue life of A508–Cl 3 steel containing 0.003 wt.% sulfur is plotted as a function of temperature and strain rate in Fig. 9. Although scatter is significant, the data indicate little or no dependence of fatigue life on temperature and strain rate. The data suggest a minimum threshold value of 0.003 wt.% sulfur in the steels below which environmental effects on fatigue life are negligible. The available data are inadequate to establish either the dependence of fatigue life on sulfur content or the upper limit for sulfur content above which the effect of sulfur on fatigue life may saturate.

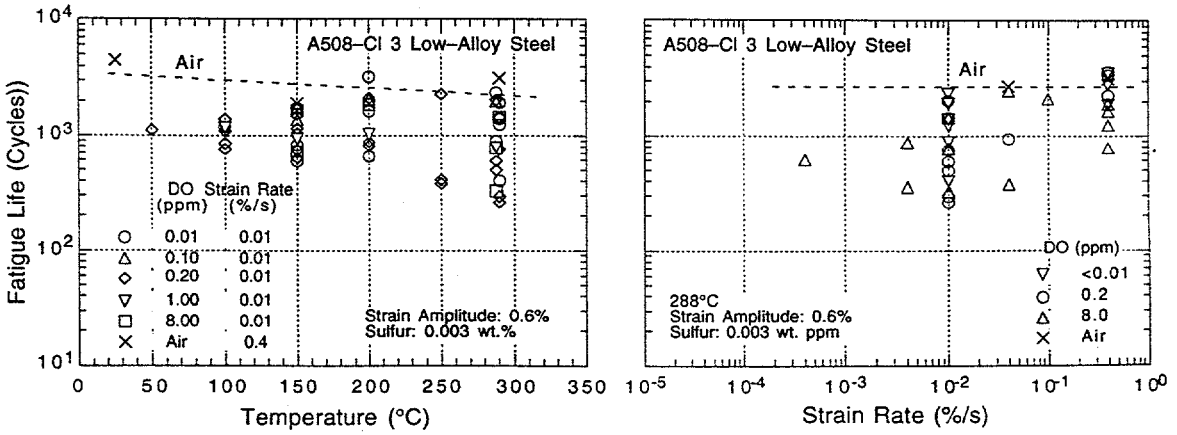

Figure 9—Dependence of fatigue life of low–alloy steels containing 0.003 wt. % sulfur on temperature and dissolved oxygen

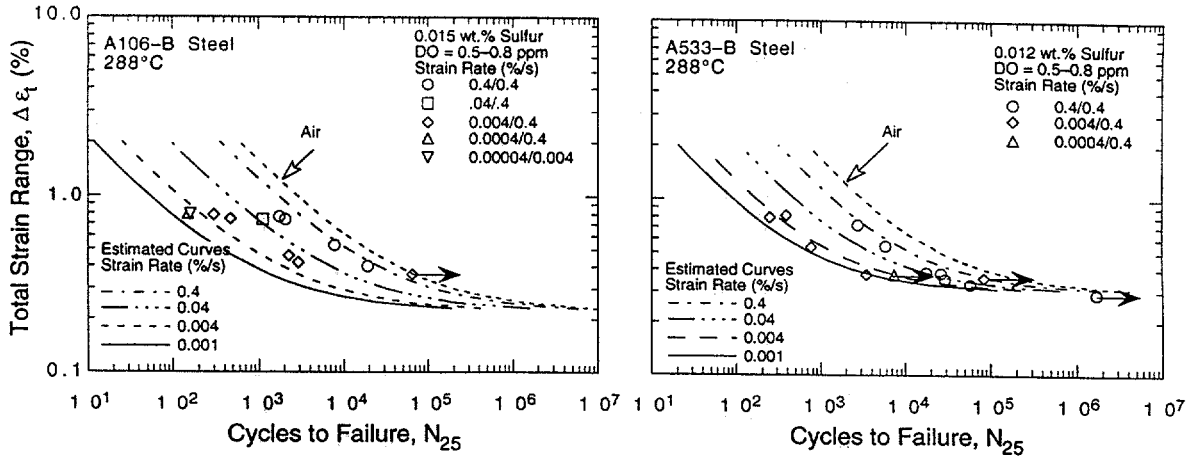

Figure 10—Fatigue S–N behavior for A106–Gr B and A533–Gr B steels estimated from model and determined experimentally in high–DO water at 288°C

Strain Amplitude

A minimum threshold strain is required for environmentally assisted decrease in fatigue life. This threshold value most likely depends both on material parameters such as amount and distribution of sulfides, and on parameters such as temperature, strain rate, and DO level in water. The fatigue life of A106–Gr B and A533–Gr B steels in high–DO water at 288°C and different strain rates is shown in Fig. 10. For these heats of carbon and low–alloy steels, the threshold strain range appears to be at ≈0.36%. This behavior is consistent with the slip–dissolution model for crack propagation [22]; the applied strain must exceed a threshold value to rupture the passive surface film in order for environmental effects to occur. However, this does not imply that the observed threshold strain is the actual film rupture strain. Film rupture occurs at the crack tip and is controlled by the crack tip strain. The threshold strain measured in smooth–specimen tests is a surrogate that in essence controls the crack tip strain, but no numerical equality between the two need be implied.

ESTIMATION OF FATIGUE LIFE

For service conditions that satisfy all critical threshold values, the fatigue life of carbon and low–alloy steels can be estimated from the statistical models [16]. The fatigue life of CSs is expressed as

$$\ln(N) = 6.186 - 1.871 \ln(\varepsilon_a - 0.11) + 0.554\, S^*\, T^*\, O^*\, \dot{\varepsilon}^* \qquad (5a)$$

and that of LASs as

$$\ln(N) = 5.901 - 1.687 \ln(\varepsilon_a - 0.15) + 0.554\, S^*\, T^*\, O^*\, \dot{\varepsilon}^*, \qquad (5b)$$

where S^*, T^*, O^*, and $\dot{\varepsilon}^*$ = transformed sulfur content, temperature, DO, and strain rate, respectively, defined as follows:

$$S^* = S \quad (0 < S \leq 0.015 \text{ wt.\%})$$
$$S^* = 0.015 \quad (S > 0.015 \text{ wt.\%}) \tag{6a}$$

$$T^* = 0 \quad (T < 150°C)$$
$$T^* = T - 150 \quad (T = 150\text{–}350°C) \tag{6b}$$

$$O^* = 0 \quad (DO < 0.05 \text{ ppm})$$
$$O^* = DO \quad (0.05 \text{ ppm} \leq DO \leq 0.5 \text{ ppm})$$
$$O^* = 0.5 \quad (DO > 0.5 \text{ ppm}) \tag{6c}$$

$$\dot{\varepsilon}^* = 0 \quad (\dot{\varepsilon} > 1 \text{ \%/s})$$
$$\dot{\varepsilon}^* = \ln(\dot{\varepsilon}) \quad (0.001 \leq \dot{\varepsilon} \leq 1 \text{ \%/s})$$
$$\dot{\varepsilon}^* = \ln(0.001) \quad (\dot{\varepsilon} < 0.001 \text{ \%/s}) \tag{6d}$$

The functional forms for S^*, T^*, O^*, and $\dot{\varepsilon}^*$ were defined on the basis of the experimental data. Equations 6b and 6d are consistent with the data in Figs. 5 and 6, respectively. In Eq. 6c, a linear rather than a logarithmic function of DO was used to define O^*. A minimum threshold value of 0.003 wt.% sulfur was not included in the model. The data suggest a linear dependence of life on sulfur content; the effect of sulfur content was assumed to saturate at 0.015 wt.% sulfur. The last term in Eqs. 5a and 5b is zero when any one of the critical threshold conditions is not satisfied, e.g., in a PWR environment the low DO would imply that environmental effects are small even for low strain rates. The fatigue life of CSs and LASs in simulated PWR water is compared with values estimated from Eq. 5 in Fig. 8. The fatigue lives in high–DO water at 288°C are compared with the estimated values in Fig. 10. The predicted fatigue lives show good agreement with the experimental results.

FATIGUE EVALUATION

The fatigue S–N correlations of Eqs. 4 and 5 show excellent agreement with data obtained under loading histories with constant strain rate, temperature, and strain amplitude. Actual loading histories are far more complex. Exploratory fatigue tests have been conducted with waveforms where the strain rate or temperature was varied during the loading cycle. The results of such tests provide guidance for developing procedures and rules for fatigue evaluation of components under complex loading histories.

Strain Rate

Exploratory fatigue tests have been conducted with waveforms where the slow strain rate is applied during only a fraction of the tensile loading cycle. Sample results for A106–Gr B steel tested in air and low– and high–DO environments at 288°C and ≈0.75% strain range are summarized in Fig. 11. The waveforms consist of segments of loading and unloading at fast and slow strain rates. The variation in fatigue life of A106–Gr B and A333–Gr 6 CSs is plotted as a function of the fraction of loading strain at slow strain rate in Fig. 12 [5–7,10]. Open symbols indicate tests where the slow portions occurred near the maximum tensile strain. Closed symbols indicate tests where the slow portions occurred near the maximum compressive strain. In Fig. 12, if the relative damage were totally independent of strain amplitude, fatigue life should decrease linearly from A to C along the chain–dot line. Instead, the results indicate that the relative

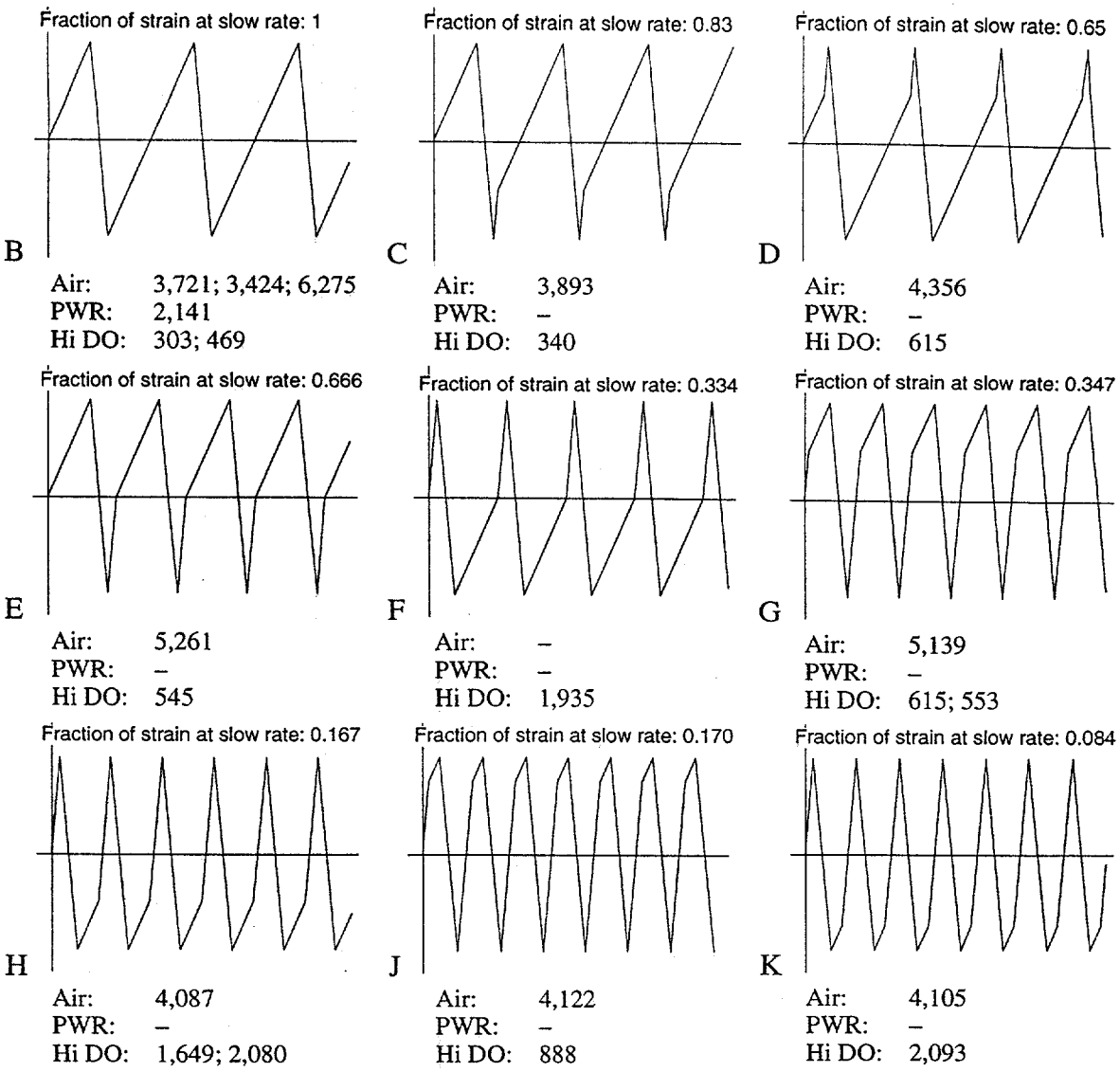

Figure 11—Fatigue life of A106–Gr B carbon steel at 288°C and 0.75% strain range in air and water environments under different loading waveforms

damage due to slow strain rate is independent of strain amplitude once the amplitude exceeds the threshold value. The threshold strain range is 0.36 % for A106–Gr B steel; a value of 0.25% was assumed for A333–Gr 6 steel. Loading histories with slow strain rate applied near maximum compressive strain (i.e., waveforms D, F, H, or K) produce no damage (line AD) until the fraction of the strain is sufficiently large that slow strain rates are occurring for strain amplitudes greater than the threshold. In contrast, loading histories with slow strain rate applied near the maximum tensile strain (i.e., waveforms C, E, G, or J) show continuous decreases in life (line AB) and then saturation when a portion of the slow strain rate occurs at amplitudes below the threshold value (line BC). For A106–Gr B steel, the decrease in fatigue life follows line ABC when a slow rate occurs near the maximum tensile strain and line ADC when it occurs near maximum compressive strain.

The A333–Gr 6 steel exhibits a somewhat different trend. For example, a slow strain rate near peak compressive strain appears to cause a significant reduction in fatigue

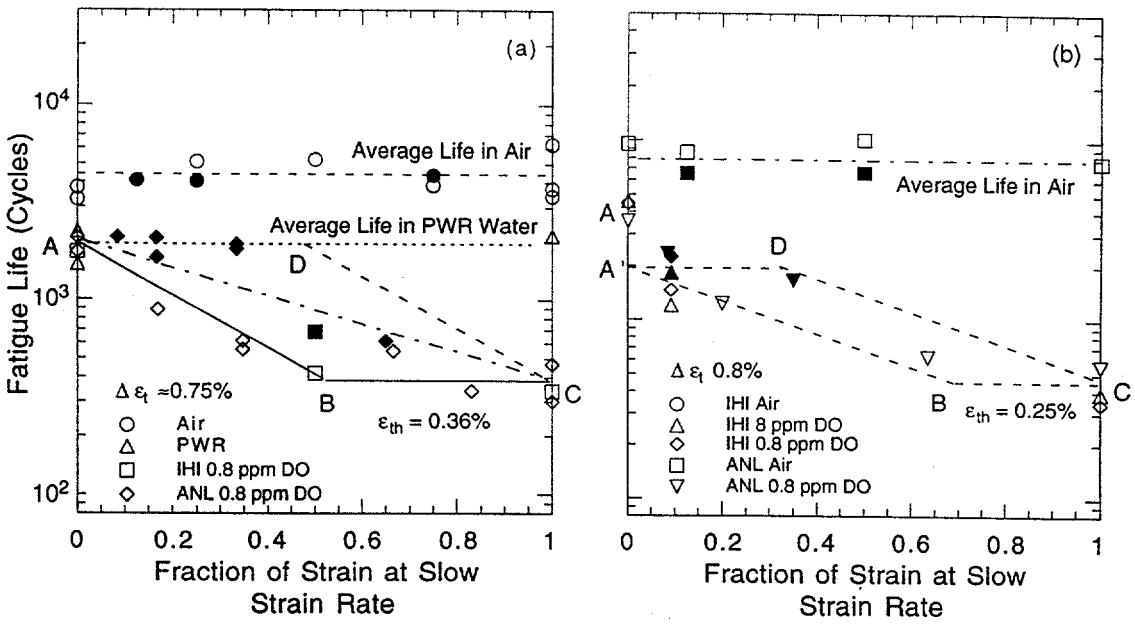

Figure 12—Fatigue life of (a) A106–Gr B and (b) A333–Gr 6 steels at 288°C tested with waveforms where slow strain rate is applied during part of tensile loading cycle. Slow strain rate (0.004%/s) occurred either near peak tensile strain (open symbols) or near peak compressive strain (closed symbols). Fast strain rate was 0.4%/s in all tests. ANL: Argonne National Laboratory and IHI: Ishikawajima–Harima Heavy Industries Co. Japan

life, while as discussed previously, slow strain rate had a significant effect on fatigue life of A106–Gr B steel only when they occurred at strains greater than the threshold strain. The apparent disagreement may be attributed to the effect of strain rate on fatigue life. This heat of A333–Gr 6 carbon steel exhibits a strain rate effect in air, e.g., fatigue life of the steel in air decreased ≈20% when the strain rate decreases from 0.4 to 0.004 %/s [7]. The cyclic hardening behavior of the steel is also quite different than that of the A106–Gr B steel. In Fig. 12, the decrease in fatigue life from A to A' is most likely caused by a strain rate effect that is independent of the environment. If the hypothesis that each portion of the loading cycle above the threshold strain is equally damaging is valid, the decrease in fatigue life due to environmental effects should follow line A'BC when a slow rate is applied near peak tensile strain, and line A'DC when it is applied near peak compressive strain. This behavior is consistent with the slip–dissolution model [22], i.e., the applied strain must exceed a threshold value to rupture the passive surface film in order for environmental effects to occur.

Temperature

Fatigue tests have been conducted on tube specimens (1 or 3 mm wall thickness) of A333–Gr 6 carbon steel in oxygenated water under combined mechanical and thermal cycling [11]. Two sequences were selected for temperature cycling: an in–phase sequence in which temperature cycling was synchronized with mechanical strain cycling, and another sequence in which temperature and strain were out of phase, i.e., maximum temperature occurred at minimum strain level and vice-versa. Three temperature ranges, 50–290°C, 50–200°C, and 200–290°C, were selected for the tests. The results are shown

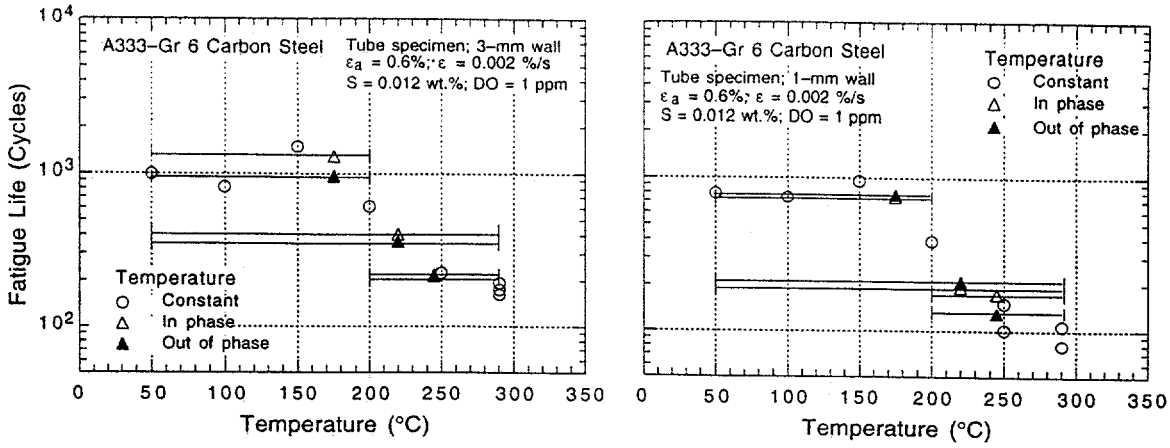

Figure 13—Effect of varying temperature on fatigue life of A333–Gr 6 carbon steel

in Fig. 13. An average temperature is used for the thermal cycling tests. Because environmental effects on fatigue life are moderate and independent of temperature below 150°C, the temperature for the tests that were cycled in the range of 50–290°C or 50–200°C was determined as the average of 150°C and the maximum temperature.

The results of constant temperature tests are consistent with the results in Fig. 5 and confirm that environmental effects on fatigue life are minimal at temperatures below 150°C. The results also indicate that the fatigue life for in–phase temperature cycling is comparable to that for out–of–phase cycling. At first glance, these results are somewhat surprising. If we consider that the tensile–loading cycle is primarily responsible for environmentally assisted reduction in fatigue life, then fatigue life for the out–of–phase tests should be longer than for the in–phase tests, because maximum strain occurs near maximum temperature for in–phase tests, whereas it occurs at temperatures below 150°C for the out–of–phase tests. As noted before, applied strain must be above a minimum threshold value for environmental effects on fatigue life. For out–of–phase tests, maximum temperatures occur at strain levels below the threshold value. If environmental effects on fatigue life are considered to be minimal at temperatures <150°C and at strain levels <0.25 %, the average temperatures for the out–of–phase tests at 50–290°C, 50–200°C, and 200–290°C temperature ranges should be 195, 160, and 236°C, respectively, instead of 220, 175, and 245°C, as plotted in Fig. 13. Consequently, the fatigue lives of out–of–phase tests are expected to be at least 50% higher than those of the in–phase tests.

The nearly identical fatigue lives for the two sequences may be explained by considering the effect of compressive–loading cycle on fatigue life. The fatigue data suggest that a slow strain rate during the compressive–loading cycle could also decrease fatigue life, although the effect of slow strain rate during a compressive cycle is smaller than that during a tensile cycle [5,10]. The thermal cycling test results shown in Fig. 13 were obtained with a triangular waveform. For out–of–phase tests, although maximum temperatures occur at strain levels that are below the threshold value for the tensile–loading cycle, they occur at maximum strain levels for the compressive–loading cycle. The contribution of compressive loading cycle on fatigue life may result in nearly the same fatigue life for in–phase and out–of–phase tests. For in–phase tests, maximum temperatures occur at strain levels that are below the threshold value for the compressive–loading cycle; contribution of compressive cycle on fatigue life would be negligible. However, the decrease in fatigue life because of a slow strain rate during compressive–loading cycle is difficult to reconcile in terms of the slip-dissolution model.

Strain Amplitude

The fatigue S–N curves specify, for a given strain or stress amplitude, the number of cycles needed to form an "engineering" crack (e.g., a 3–mm–deep crack). These allowable number of cycles may be divided into two stages: cycles for formation of microcracks (a few micrometers deep) on the surface, and cycles for propagation of the shallow surface cracks to an engineering size. The reduction in fatigue life in LWR environments may arise from a decrease in the period for formation of surface cracks and/or an increase in growth rates of the microcracks. The former is quite sensitive to applied strain amplitude.

The fatigue crack growth behavior of ferritic steels in high–temperature oxygenated water and the effects of sulfur content and loading rate are well known [23–27]. Dissolution of MnS inclusions changes the water chemistry near the crack tip, making it more aggressive. This results in enhanced crack growth rates because either (a) the dissolved sulfides decrease the repassivation rate, which increases the amount of metal dissolution for a given oxide rupture rate [23]; or (b) the dissolved sulfide poisons the recombination of H atoms liberated by corrosion, which enhances H uptake by the steel at the crack tip [27]. In addition to the effects of environment on crack growth, the water environment may also enhance crack nucleation. For example, corrosion pits or cavities produced by dissolution of MnS inclusions can act as sites for nucleation of fatigue cracks.

All fatigue specimens tested in water show surface micropitting. The specimens also contain an abundance of surface cracks, their surface length may vary from <10 to several hundred micrometers. These cracks may consist of several cracks that formed at different sites and then merged, or they may represent a single crack. A detailed evaluation of the test specimens did not show any evidence that fatigue cracks form preferentially at the micropits [28]. Examination of the fatigue specimens indicates that irrespective of environment, cracks in carbon and low–alloy steels form along slip bands, carbide particles, or at the ferrite/pearlite phase boundaries. The cracking frequency, defined as the number of cracks along longitudinal sections of the gauge length, for fatigue specimens tested in different environments has also been measured [28]. The results show that environment has no effect on the frequency of cracking. For similar loading conditions, the number of cracks in the specimens tested in air and oxygenated water with 0.8 ppm DO are identical, although fatigue life in water is lower by a factor of ≈8. If the reduction in life is due to an enhancement in the formation of surface microcracks, the specimens tested in high DO water should show more surface cracks.

Exploratory tests have also been conducted to evaluate the contributions of environment to the formation of surface microcracks. Figure 14 shows the fatigue life of A106–Gr B steel in air (dashed line) and in high–DO water at 0.4 and 0.004%/s strain rates (circle and diamond symbols, respectively). Fatigue tests were conducted on specimens that were preexposed at 288°C for 30–100 h in water with 0.6–0.8 ppm DO and then tested either in air or <10 ppb DO water. At 0.4% strain range, nearly half the fatigue life may be spent in the formation of surface cracks. Fatigue lives of the preoxidized specimens are identical to those of nonoxidized specimens; life would be expected to decrease if surface micropits facilitate surface cracking. Preoxidized specimens of A533–Gr B low–alloy steel also show a similar behavior. Sequential tests have been conducted to check the possibility that both the high DO and slow strain rate are required to influence surface cracking. Fatigue specimens were first tested in high–DO water at 0.4% strain range and 0.004%/s strain rate for 570 cycles (≈25% of the life at these loading conditions) and then tested in either air or high–DO water at 0.4%/s strain rate. Fatigue life of these tests should be lower if formation of surface cracks

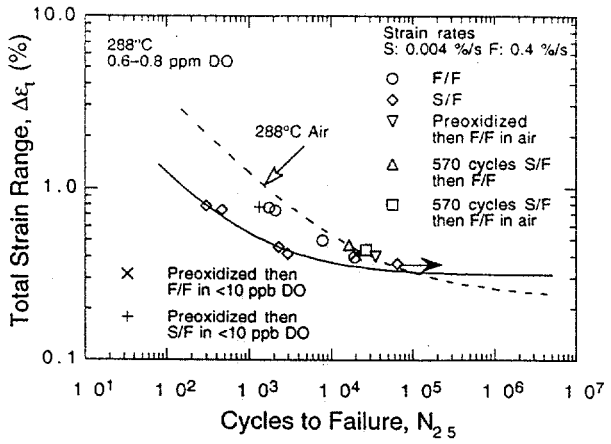

Figure 14—
Environmental effects on formation of surface microcracks. Preoxidized specimens were exposed at 288°C for 30–100 h in water with 0.6–0.8 ppm DO.

contributes in any way to environmental effects. Once again, no reduction in life is observed; the tests yield a CUF value of >1. These results suggest that the reduction in fatigue life in high–DO water is primarily due to environmental effects on fatigue crack propagation.

CONCLUSIONS

The available data on the effects of various material and loading variables such as steel type, orientation, dissolved oxygen level, strain range, strain rate, loading waveform, and surface morphology on the fatigue life of carbon and low–alloy steels in air and water environments have been summarized. In air, the fatigue life of carbon and low–alloy steels depends on steel type, temperature, orientation (rolling or transverse), and strain rate. The fatigue life of CSs is a factor of ≈1.5 lower than that of LASs. For both steels, fatigue life decreases with increase in temperature up to 320°C. Strain rate and orientation are important in some heats of CSs and LASs. For these heats, fatigue life decreases with decreasing strain rate. Also, the fatigue properties in transverse orientation may be inferior to those in the rolling orientation. Structural factors, e.g., distribution and morphology of sulfides, are responsible for the poor fatigue resistance in transverse orientations. In an air environment, the fatigue S–N curves for carbon and low–alloy steels indicate significant heat–heat–variation. At 288°C, fatigue life may vary up to a factor of 5 above or below the mean value. The results also indicate that the ASME mean curve for CSs is somewhat conservative with respect to the experimental data; at strain amplitudes <0.2%, the mean curve predicts significantly lower fatigue lives than those observed experimentally. The ASME mean curve for LASs shows good agreement with the experimental data.

Both carbon and low–alloy steels exhibit dynamic strain aging at temperatures between 200–370°C, which leads to enhanced cyclic hardening, a secondary hardening stage, and negative strain rate sensitivity, i.e., cyclic stress increases with decreases in strain rate. The temperature range and extent of dynamic strain aging vary with compositional and structural factors. The large variation in fatigue life that has been observed in the tests at 288°C may be due to differences in the extent of dynamic strain aging in the steel.

The available fatigue strain vs. life (S–N) data in LWR environments suggest that the reduction in fatigue life in high–DO water is primarily due to environmental effects

on the growth of shallow cracks. The results show that environmental effects on fatigue life are significant when five conditions are satisfied simultaneously, viz., applied strain range, temperature, dissolved oxygen in water, and sulfur content in steel are above a minimum threshold level, and strain rate is below a critical value. Although the structure and cyclic–hardening behavior of carbon and low–alloy steels are distinctly different, there is little or no difference in susceptibility to environmental degradation of fatigue life of these steels. The fatigue life of carbon and low–alloy steels in air and LWR environments can be estimated from the statistical models.

For both steels, the fatigue data indicate threshold values of 150°C for temperature, 0.05 ppm for DO, and 0.003 wt.% for sulfur, above which fatigue life is decreased significantly in LWR environments if the other two threshold conditions are also satisfied. At 150–320°C, fatigue life decreases linearly with temperature. The effect of DO content on life saturates at 0.5 ppm; higher DO levels do not cause further decreases in fatigue life. For DO levels between 0.05 and 0.5 ppm, the fatigue life may be represented equally well by either a linear or logarithmic dependence of life on DO content. The data indicate a maximum threshold value of 1%/s for strain rate below which environmental effects on life are significant. When the threshold conditions for all five parameters are satisfied, fatigue life decreases logarithmically with decreasing strain rate. The effect of strain rate on life saturates at ≈0.001%/s strain rate. The existing fatigue data are inadequate to establish the dependence of fatigue life on sulfur content, or to define the saturation level. The minimum threshold value for strain also can not be defined from the existing fatigue data. Most likely it depends on material parameters, e.g., size and distribution of sulfides, and on service parameters, e.g., temperature, strain rate, and DO level in water. Limited data suggest that the threshold strain is either equal to or slightly greater than the endurance limit of the material.

Only a moderate decrease in fatigue life is observed in LWR environments when any one of the threshold conditions is not satisfied, e.g., at temperatures ≤150°C, or in low–DO PWR environments (≤0.05 ppm DO), or for low–sulfur steels (containing ≤0.003 wt.% sulfur). Under these conditions, life in water is 30–50% lower than that in air. The effects of orientation and strain rate are similar to those in air. For example, in a PWR environment at 288°C, heats of steel that are sensitive to strain rate also show a decrease in life as strain rate decreases, whereas heats that are not sensitive to strain rate do not show a change in life even when strain rate decreases by three orders of magnitude.

In LWR environments, when all of the threshold conditions are satisfied, both the tensile– and compressive–loading cycles are responsible for environmentally assisted reduction in fatigue life, although the effect of the compressive cycle is smaller than that of the tensile cycle. For loading cycles in which strain rate and temperature also vary with strain, the results indicate that environmental effects on fatigue life occur only when the five threshold conditions are satisfied. For example, a slow strain rate is effective in decreasing fatigue life only when it occurs at strains greater than the threshold strain. Also, slow strain rates applied during any portion of the loading cycle above the minimum threshold strain are equally effective in decreasing life. The fatigue S–N behavior for loading cycles where both temperature and strain change may be represented by an average temperature, determined from only that portion of the cycle where all five threshold conditions are satisfied. Limited data suggest that a linear summation of individual usage factors to determine CUF for a location is applicable for LWR environments; the results of sequential loading tests yield CUF values of ≥1, i.e., the linear damage model is conservative. However, additional data are needed to verify these results.

ACKNOWLEDGMENTS

This work was supported by the Office of Nuclear Regulatory Research of the U.S. Nuclear Regulatory Commission, FIN Number A2212; Program Manager: Dr. M. McNeil.

REFERENCES

1. B. F. Langer, Design of Pressure Vessels for Low–Cycle Fatigue, ASME J. of Basic Engineering **84** (1962) 389–402.

2. D. A. Hale, S. A. Wilson, J. N. Kass, and E. Kiss, *Low Cycle Fatigue Behavior of Commercial Piping Materials in a BWR Environment,* J. Eng. Mater. Technol. **103**, 15–25 (1981).

3. S. Ranganath, J. N. Kass, and J. D. Heald, *Fatigue Behavior of Carbon Steel Components in High–Temperature Water Environments*, in Low–Cycle Fatigue and Life Prediction, ASTM STP 770, C. Amzallag, B. N. Leis, and P. Rabbe, eds., American Society for Testing and Materials, Philadelphia, PA, pp. 436–459 (1982).

4. J. B. Terrell, *Effect of Cyclic Frequency on the Fatigue Life of ASME SA–106–B Piping Steel in PWR Environments*, J. Mater. Eng. **10**, 193–203 (1988).

5. O. K. Chopra and W. J. Shack, *Effects of LWR Environments on Fatigue Life of Carbon and Low–Alloy Steels*, in Fatigue and Crack Growth: Environmental Effects, Modeling Studies, and Design Considerations, PVP Vol. 306, S. Yukawa, ed., American Society of Mechanical Engineers, New York, pp. 95–109 (1995).

6. O. K. Chopra and W. J. Shack, *Effects of Material and Loading Variables on Fatigue Life of Carbon and Low–Alloy Steels in LWR Environments*, in Transactions of 13th Int. Conf. on Structural Mechanics in Reactor Technology (SMiRT 13), Vol. II, M. M. Rocha and J. D. Riera, eds., Escola de Engenharia – Universidade Federal do Rio Grande do Sul, Porto Alegre, Brazil, pp. 551–562 (1995).

7. O. K. Chopra, D. J. Gavenda, and W. J. Shack, in *Environmentally Assisted Cracking in Light Water Reactors, Semiannual Report, October 1994–March 1995,* NUREG/CR–4667 Vol. 20, ANL–95/41, pp. 1–19 (Jan. 1996).

8. M. Higuchi and K. Iida, *Fatigue Strength Correction Factors for Carbon and Low–Alloy Steels in Oxygen–Containing High–Temperature Water,* Nucl. Eng. Des. **129**, 293–306 (1991).

9. N. Nagata, S. Sato, and Y. Katada, *Low–Cycle Fatigue Behavior of Low–Alloy Steels in High–Temperature Pressurized Water*, in Transactions of 10th Int. Conf. on Structural Mechanics in Reactor Technology, F. A. H. Hadjian, ed., American Association for Structural Mechanics in Reactor Technology, Anaheim, CA (1989).

10. M. Higuchi, K. Iida, and Y. Asada, *Effects of Strain Rate Change on Fatigue Life of Carbon Steel in High–Temperature Water*, in Fatigue and Crack Growth: Environmental Effects, Modeling Studies, and Design Considerations, PVP Vol.

306, S. Yukawa, ed., American Society of Mechanical Engineers, New York, pp. 111–116 (1995).

11. H. Kanasaki, M. Hayashi, K. Iida, and Y. Asada, *Effects of Temperature Change on Fatigue Life of Carbon Steel in High Temperature Water*, in Fatigue and Crack Growth: Environmental Effects, Modeling Studies, and Design Considerations, PVP Vol. 306, S. Yukawa, ed., American Society of Mechanical Engineers, New York, pp. 117–122 (1995).

12. G. Nakao, H. Kanasaki, M. Higuchi, K. Iida, and Y. Asada, *Effects of Temperature and Dissolved Oxygen Content on Fatigue Life of Carbon and Low–Alloy Steels in LWR Water Environment*, in Fatigue and Crack Growth: Environmental Effects, Modeling Studies, and Design Considerations, PVP Vol. 306, S. Yukawa, ed., American Society of Mechanical Engineers, New York, pp. 123–128 (1995).

13. H. Choi, S. Smialowska, and D. D. Macdonald, *Effect of Fluid Flow on the Stress Corrosion Cracking of ASME SA508–Cl2 Steel and AISI Type 304 Stainless Steel in High Temperature Water*, in The General and Localized Corrosion of Carbon and Low–Alloy Steels in Oxygenated High–Temperature Water, EPRI NP–2853, Electric Power Research Institute, Palo Alto, CA (Feb. 1983).

14. E. Lenz, N. Wieling, and H. Munster, *Influence of Variation of Flow Rates and Temperature on the Cyclic Crack Growth Rate under BWR Conditions*, in Proc. 3rd Intl. Symp. on Environmental Degradation of Materials in Nuclear Power Systems – Water Reactors, G. J. Theus and J. R. Weeks, eds., The Metallurgical Society, Warrendale, PA. pp. 283–288 (1988).

15. S. Majumdar, O. K. Chopra, and W. J. Shack, *Interim Fatigue Design Curves for Carbon, Low–Alloy, and Austenitic Stainless Steels in LWR Environments*, NUREG/CR–5999, ANL–93/3 (April 1993).

16. J. Keisler, O. K. Chopra, and W. J. Shack, *Fatigue Strain–Life Behavior of Carbon and Low–Alloy Steels, Austenitic Stainless Steels, and Alloy 600 in LWR Environments*, NUREG/CR–6335, ANL–95/15 (Aug. 1995).

17. W. A. Van Der Sluys and S. Yukawa, *Status of PVRC Evaluation of LWR Coolant Environmental Effects on the S–N Fatigue Properties of Pressure Boundary Materials*, in Fatigue and Crack Growth: Environmental Effects, Modeling Studies, and Design Considerations, S. Yukawa, ed., American Society of Mechanical Engineers, New York, pp. 47–58 (1995).

18. H. Abdel–Raouf, A. Plumtree, and T. H. Topper, *Effects of Temperature and Deformation Rate on Cyclic Strength and Fracture of Low–Carbon Steel*, in Cyclic Stress–Strain Behavior – Analysis, Experimentation, and Failure Prediction, ASTM STP 519, American Society for Testing and Materials, Philadelphia, PA., pp. 28–57 (1973).

19. K. Tsuzaki, Y. Matsuzaki, T. Maki, and I. Tamura, *Fatigue Deformation Accompanying Dynamic Strain Aging in a Pearlitic Eutectoid Steel*, Mater. Sci. and Eng. **A142**, 63–70 (1991).

20. B. H. Lee and I. S. Kim, *Dynamic Strain Aging in the High–Temperature Low–Cycle Fatigue of SA 508 Cl. 3 Forging Steel*, J. Nucl. Mater. **226**, 216–225 (1995).

21. L. A. James, *The Effect of Temperature and Cyclic Frequency Upon Fatigue Crack Growth Behavior of Several Steels in an Elevated Temperature Aqueous Environment,* J. Pressure Vessel Technol. **116**, 122–127 (1994).

22. F. P. Ford, S. Ranganath, and D. Weinstein, *Environmentally Assisted Fatigue Crack Initiation in Low–Alloy Steels – A Review of the Literature and the ASME Code Design Requirements*, EPRI Report TR–102765 (Aug. 1993).

23. F. P. Ford and P. L. Andresen, *Stress Corrosion Cracking of Low–Alloy Pressure Vessel Steel in 288°C Water*, in Proc. 3rd Int. Atomic Energy Agency Specialists' Meeting on Subcritical Crack Growth, NUREG/CP–0112, Vol. 1, pp. 37–56 (Aug. 1990).

24. P. M. Scott and D. R. Tice, *Stress Corrosion in Low–Alloy Steels*, Nucl. Eng. Des. **119**, 399–413 (1990).

25. W. H. Cullen, *The Effects of Sulfur Chemistry and Load Ratio on Fatigue Crack Growth Rates in LWR Environments*, in Proc. 2nd Int. Atomic Energy Agency Specialists' Meeting on Subcritical Crack Growth, NUREG/CP–0067, MEA–2090, Vol. 2, pp. 339–355 (April 1986).

26. J. H. Bulloch, *A Review of the Fatigue Crack Extension Behavior of Ferritic Pressure Vessel Materials in Pressurized Water Reactor Environments*, Res. Mechanica, **26**, 95–172 (1989).

27. T. F. Kassner, W. J. Shack, W. E. Ruther, and J. H. Park, *Environmentally Assisted Cracking of Ferritic Steels*, in Environmentally Assisted Cracking in Light Water Reactors: Semiannual Report, April–September 1990, NUREG/CR–4667, Vol. 11, ANL–91/9, pp. 2–9 (May 1991).

28. O. K. Chopra, W. F. Michaud, W. J. Shack, and W. K. Soppet, in *Environmentally Assisted Cracking in Light Water Reactors, Semiannual Report, April–September 1993*, NUREG/CR–4667 Vol. 17, ANL–94/16, pp. 1–22 (June 1994).